Environment-Dependent Photophysics of Polymer-Bound J Aggregates Determined by Time-Resolved Fluorescence Spectroscopy and Time-Resolved Near-Field Scanning Optical Microscopy

Philip J. Reid,[†] Daniel A. Higgins, and Paul F. Barbara*

Department of Chemistry, University of Minnesota, Minneapolis, Minnesota 55455

Received: October 12, 1995; In Final Form: December 7, 1995[⊗]

Exciton migration and annihilation dynamics in J aggregates comprised of a pseudoisocyanine (PIC) dye and poly(vinyl sulfate) (PVS) are studied by time-correlated, single-photon-counting (TCSPC) methods coupled with near-field scanning optical microscopy (TCSPC-NSOM) and also by conventional, far-field TCSPC. Far-field TCSPC studies of the aggregates in aqueous solution demonstrate that the exciton lifetime in the absence of annihilation (at low excitation intensities) is 789 ± 36 ps with biexponential exciton decay occurring at high excitation intensities due to exciton annihilation. Analysis of the intensity-dependent decay with conventional exciton decay theories demonstrates that the observed decay dynamics are consistent with exciton migration limited to finite molecular domains. In contrast to the solution studies, deposition of a thin PIC/PVS aggregate film onto fused quartz results in a dramatic reduction in the exciton lifetime to ∼10 ps. This lifetime demonstrates only modest dependence on excitation intensity. Possible mechanisms for the reduction in exciton lifetime for the adsorbed aggregates are discussed. Finally, the dependence of the exciton lifetime on the nanostructure of the aggregates is explored with TCSPC-NSOM. A new TCSPC-NSOM instrument with an instrument response of 30 ps and spatial resolution of ∼100 nm is presented and used to perform the first direct measurement of exciton lifetimes for a **single** aggregate. TCSPC-NSOM studies demonstrate that the exciton lifetime is not sensitive to the structural details of the aggregates on the ∼100 nm length scale. The combination of measurements presented here demonstrate that the exciton diffusion length is limited to short distances (∼100 nm) relative to the aggregate size. The homogeneous spectral properties observed for these aggregates are therefore not due to site-averaging resulting from long-range exciton migration but instead are due to the structural homogeneity of the aggregates on the length scales investigated here.

Introduction

Aggregated molecular structures have attracted much interest due to their unique electronic and physical properties relative to those of their monomeric constituents.[1−3] A particularly interesting class of molecular aggregates is comprised of those formed by pseudoisocyanine (PIC) dyes which have found wide application in the sensitization of photographic materials and have served as a model for photosynthetic antenna pigments.[2−7] The distinguishing characteristic of PIC aggregates is the red-shifting and narrowing of the lowest energy transition relative to that of monomeric PIC upon aggregation. This electronic transition, known as the J-band, corresponds to a delocalized, excitonic state of the aggregate created by electronic coupling of neighboring dye molecules. Due to coupling with aggregate phonons, the number of monomers which may participate in this delocalized state is limited to between 4 and 20 molecules.[7−10] Interaction of the molecular excitations and long-distance migration of the exciton, corresponding to the transfer of energy from one set of coupled chromophores to a neighboring set, is thought to result in the observed homogeneity of the aggregate emission.[11,12]

Although extensive experimental and theoretical work has centered on the study of PIC aggregates, measurements designed to probe the structural dependence of the photophysical properties of these aggregates have only recently been performed. Nonspectroscopic microscopies, such as SEM[13] and AFM,[14] have been utilized to study the structural aspects of these aggregates. However, much of the current understanding of PIC aggregate photophysics has been derived from far-field optical spectroscopy; therefore, our laboratory has recently applied near-field scanning optical microscopy (NSOM) to study the spectroscopic properties of molecular aggregates with spatial resolution of ∼100 nm.[12,15] NSOM provides spatial resolution beyond the diffraction limit of conventional optical microscopies while maintaining the optical capabilities critical in characterizing the photophysical properties of materials.[16−29] Previous NSOM studies of PIC aggregates have provided information on the nanometric structure of the aggregates as well as the length scale for exciton migration.[12,15] One of the most interesting conclusions to come from this work was that in contrast to the conventional picture of exciton migration, photochemical hole-burning of the aggregates suggests that the diffusion length of the exciton is relatively limited (≤50 nm).[12] However, the direct study of exciton migration necessitates the implementation of time-resolved spectroscopic techniques.

In this paper, we investigate the environmental dependence of PIC aggregate photophysics utilizing time-correlated, single-photon-counting (TCSPC) techniques in both NSOM studies (TCSPC-NSOM) of the aggregates and in conventional, far-field studies. With far-field TCSPC, the exciton decay time for PIC aggregates grown in aqueous poly(vinyl sulfate) (PVS) solution is found to be 789 ± 36 ps at low excitation intensities in agreement with previous studies of PIC aggregates in aqueous solution.[30,31] At high intensities, exciton annihilation is ob-

* To whom correspondence should be addressed.
[†] Present address: Dept. of Chemistry, University of Washington, Seattle, WA 98195.
[⊗] Abstract published in *Advance ACS Abstracts,* February 15, 1996.

0022-3654/96/20100-3892$12.00/0

served, resulting in biexponential decay kinetics. The intensity-dependent exciton decay kinetics are compared to contemporary exciton decay theories and are found to be consistent with confinement of the excitons to finite domains. In contrast, thin films of the PIC/PVS aggregates on fused quartz demonstrate different photophysics with an exciton decay time of only ~10 ps. The fast exciton decay time for the aggregates on fused quartz required improvement in the time resolution of current TCSPC-NSOM technology;[20,24] therefore, we have incorporated a multichannel plate for detection, resulting in improvement of the instrument response to 30 ps. Studies utilizing the new TCSPC-NSOM instrument demonstrate that the exciton decay time is not sensitive to the structural details of a particular aggregate. In combining far-field and near-field TCSPC results, the exciton diffusion length is estimated to be ~100 nm, demonstrating that the homogeneity of the aggregate emission is not due to long-range exciton migration but is instead due to the homogeneous structure of the aggregates on the ~100 nm length scale.

Experimental Section

J aggregates were grown according to the following procedure. A 0.2 mL aliquot of a 10 mM stock solution of the pseudoisocyanine (PIC) dye 1,1′-diethyl-2,2′-cyanine iodide (Aldrich) in spectrophotometric grade methanol (Fisher) was added to a stirring solution of 30 mg of poly(vinyl sulfate), potassium salt (PVS, Aldrich) dissolved in 3 mL of distilled water heated to 90 °C. A fresh dye solution was made for every aggregate preparation since older stock solutions produced J aggregates with exciton decay kinetics different from those reported here. The PIC/PVS solution was then used for the time-correlated, single-photon-counting experiments described below. For the near-field scanning optical microscopy (NSOM) experiments, the PIC/PVS solution was deposited on a 200-μm-thick fused-quartz microscope cover slip by spin-coating. A hot pipet was used to transfer an aliquot of the aggregate solution to a cover slip mounted on the spin coater and the cover slip was spun at 2000 rpm until a dry surface was obtained. All samples were kept in the dark until use.

The time-correlated, single-photon-counting (TCSPC) apparatus consisted of a mode-locked Nd:YAG laser (Quantronix 116) which synchronously pumped a single-jet dye laser (Coherent 702) employing rhodamine 6G in ethylene glycol. The dye laser output at 570 nm consisted of 6 ps pulses with an average output power of 100 mW. The 76 MHz repetition rate of this laser was reduced to 4 MHz and an average power of 2 mW with a Bragg diffraction crystal (Camac Model 5000 driver coupled to a Harris TeO_2 Bragg crystal) placed external to the dye-laser cavity. The 4 MHz output was utilized as the excitation source for the TCSPC experiments; variation of the light intensity in all experiments was accomplished with reflective neutral density filters. The beam was weakly focused (300 μm diameter) onto the front face of a 2 mm cuvette containing the sample. Fluorescence was collected from the front face of the cuvette and delivered to a multichannel plate (MCP, Hamamatsu multi-alkali) biased at −3200 V. In separate experiments, fluorescence was also collected at 90°, resulting in kinetics identical with those obtained with the front-face arrangement, provided the beam was positioned close to the collection side of the cuvette to minimize artifacts arising from absorption and reemission.[10,32] Far-field TCSPC experiments on the film samples were performed by replacing the cuvette with the fused-quartz cover slip and collecting the fluorescence from the front face. The signal from the MCP was preamplified and sent to a constant-fraction discriminator (Tennelec Model 454), the output of which served as the start pulse in reverse-timing mode for the time-to-amplified converter (TAC, EG&G Ortec Model 457). The stop pulse was provided by a diode monitoring the pulse-selected dye laser output with this signal delivered to one of the discriminator inputs operating in leading-edge mode. The output of the TAC was sent to a multichannel analyzer (Tracor Northern Model 7200). The instrument response was obtained by detecting the scattering from a colloidal suspension or from a spin-coated sample of the colloidal suspension on a microscope cover slip depending on the state of the sample being investigated. Either technique provided an instrument response with a full width at half-maximum (fwhm) of 25 ps. Finally, calibration of the appratus was performed with a fixed, 3 ns delay provided by a BNC cable, a discrete delay box (Canberra Model 2058), and by misaligning the pulse selector producing satellite pulses with a time separation determined by the repetition rate of the dye laser. All three techniques resulted in identical calibrations.

Near-field scanning optical microscopy (NSOM) was performed with a commercial instrument (Topometrix Aurora) modified as described previously with the exception of the detector.[12] The low-bias avalanche photodiode previously employed[24] was replaced with a MCP to improve the time-resolution of the instrument for TCSPC with the output of the MCP manipulated as described above. The pulse-selected output of the dye laser was delivered to the microscope via a 6 m optical fiber and then coupled into the NSOM tip. A bandpass filter was placed after the 6 m fiber to reject Raman scattering originating in the fiber. This combination of excitation and detection resulted in an instrument response function fwhm of 30 ps as determined by scattering from a PVS-covered microscope cover slip surface in the absence of imbedded aggregates. This new detection scheme results in a 4-fold improvement in time resolution over current TCSPC-NSOM designs.[24]

Results and Discussion

To better understand the excited-state dynamics observed in near-field scanning optical microscopy (NSOM), the dynamics of the PIC/PVS aggregates in bulk solution, and on fused silica cover slips were characterized with far-field TCSPC. The results from this study will be prsented first, followed by the results from the TCSPC-NSOM investigation.

PIC Aggregates in Solution. Figure 1 presents the time-resolved fluorescence from a solution of the PIC/PVS aggregates at low and high excitation intensity. At low intensity (Figure 1A), the decay was well modeled by a convolution of the instrument response with a single-exponential resulting in an excited-state decay time constant of 789 ± 36 ps. The goodness of fit was evaluated by inspection of the residuals and the reduced χ^2.[33] This time constant is in agreement with previous results for PIC aggregates formed in aqueous solution.[30,31] As the laser intensity is increased (Figure 1B), the fluorescence decay becomes biphasic with a fast component of 79 ± 10 ps at all powers investigated except at 5.7×10^{11} photons/cm^2 pulse where reduction of this time constant to 43 ± 8 ps was observed. At all excitation intensities, the slow component of the decay was identical to that observed at low power. Figure 2 presents the normalized amplitude for the fast and slow decay components as a function of excitation intensity demonstrating the power-dependent evolution from single- to double-exponential exciton decay. This result stands in contrast to previous studies of PIC J aggregates in PVS where an intensity independent excited-state decay time of 17 ± 3 ps was observed.[10] However, the aggregates in this earlier experiment were generated at a

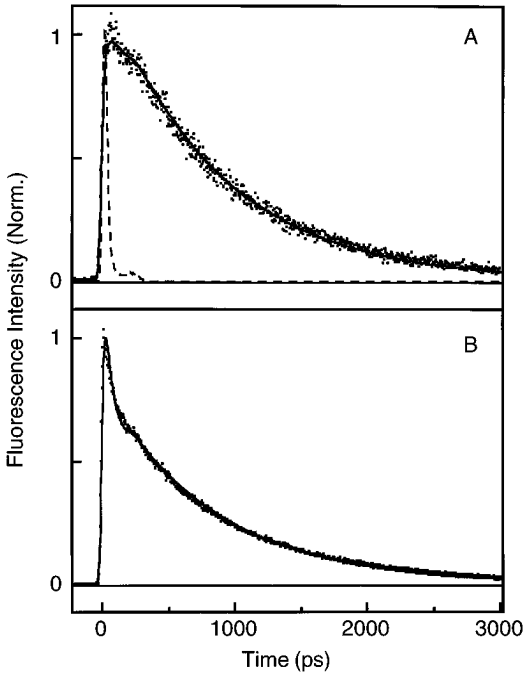

Figure 1. (A) Fluorescence decay curve obtained from a solution of PIC J aggregates in poly(vinyl sulfate) obtained with an intensity of 1×10^8 photons/cm^2 pulse. The instrument response is given by the dashed curve. The solid line through the points is the fit to a convolution of the instrument response with a single-exponential resulting in an excited-state decay time of 789 ± 36 ps. (B) Identical to A except that the excitation intensity was 5.7×10^{11} photons/cm^2 pulse. Evolution from single to double-exponential decay kinetics is evident.

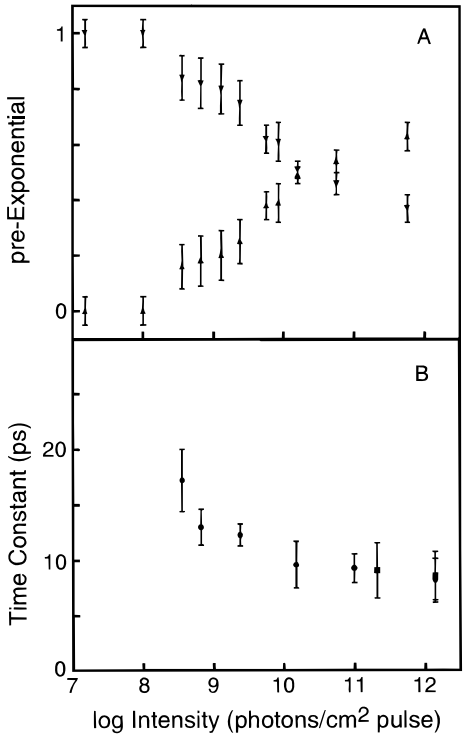

Figure 2. (A) Evolution in the preexponential coefficients as a function of power. The data were fit to a convolution of the instrument response with a sum of two exponentials with decay times of 789 ± 36 and 79 ± 10 ps. The preexponential for the 789 ps component is given by inverted triangles and coefficients for the 79 ps component are given by the regular triangles. (B) Power dependence of the excited-state decay time for PIC/PVS aggregates on a fused-quartz cover slip. The points correspond to TCSPC (circles) and TCSPC-NSOM (squares) with the power determined by measurement in the far field.

dye to polymer ratio roughly 100 times larger than the aggregates investigated here. In recent NSOM investigations we have observed that aggregate structure is very preparation dependent; therefore, the apparent discrepancy between the results presented here and in previous studies may simply be related to differences in aggregate structure.[34,35]

Deviation from single-exponential decay kinetics at high excitation intensity has been observed and assigned to exciton annihilation.[30,36,37] Here, exciton annihilation (also referred to as exciton fusion) refers to the following process:

$$S_1 + S_1 \rightarrow S_1 + S_0 \tag{1}$$

where two singlet, excited-state excitons (S_1) interact to produce a single, excited exciton. Other annihilation processes involving triplet excitons are possible; however, we will consider only singlet exciton annihilation here. The kinetics of exciton decay in the presence of annihilation have been modeled with three different theories which are outlined below and compared to our experimental results.

Binary Collision Theory. This theory was originally applied to the exciton-decay dynamics of PIC aggregates in aqueous solution by Brumbaugh et al.[31] There are two major assumptions in this treatment. First, the domain over which the excitons migrate is assumed to be sufficiently large such that the exciton density remains constant. Second, the migration of the excitons is assumed to be faster than the rate of single-exciton decay; therefore, a stochastic distribution of excitons over the domain is maintained. In this limit, the exciton decay is described by the differential equation

$$\frac{\partial[\mathrm{N}]}{\partial t} = -k[\mathrm{N}] - \frac{\gamma}{2}[\mathrm{N}]^2 \tag{2}$$

where [N] is the concentration of excitons, k is the single exciton decay rate, and γ is the exciton annihilation rate. As has been noted previously, this equation predicts that the decay kinetics should be Markovian in that the slope of the fluorescence decay curve should depend only on the number of excitons present and not on the history of the decay.[37] Comparison of the slope of the fluorescence decay curves obtained with two different excitation intensities at times where the fluorescence intensity is identical (i.e., the same number of excitons) reveals that the curves do not have the same slope (Figure 3). Therefore, the exciton decay kinetics demonstrate non-Markovian behavior with the rate of decay dependent on both the time evolution of the exciton decay and the exciton concentration. As expected, a full analysis employing binary collision theory was incapable of reproducing the intensity-dependent exciton decay.

Exciton Migration in Reduced Dimensions and Static Annihilation. Exciton migration confined to reduced dimensions (i.e., sub-3-dimensional) as well as exciton annihilation via static, long-range Förster interaction leads to the following rate equation for exciton decay:[37−40]

$$\frac{\partial[\mathrm{N}]}{\partial t} = -k[\mathrm{N}] - \frac{\gamma}{2}t^{-h}[\mathrm{N}]^2 \tag{3}$$

where, in the reduced dimensionality treatment, h is related to the dimensionality by:

$$h = 1 - d_f/2 \tag{4}$$

where d_f is the dimensionality ($1 \leq d_f < 2$). This equation has been used to describe the migration of triplet excitons in fractal dimensions[38] as well as the one-dimensional exciton annihilation

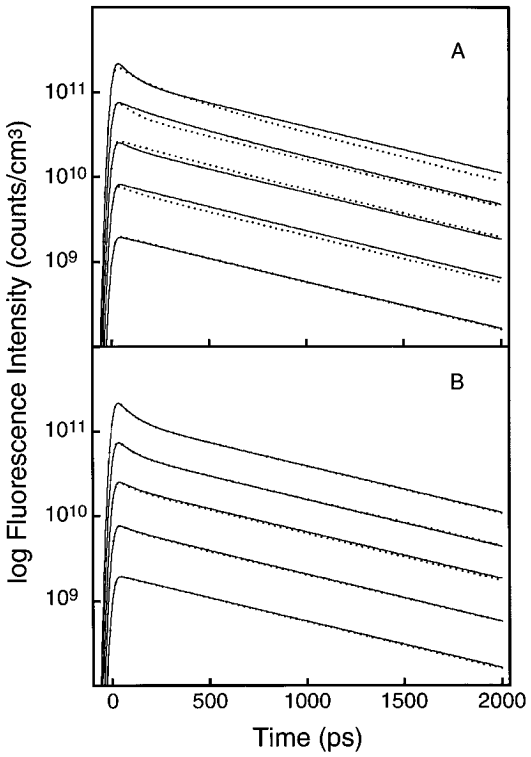

Figure 3. (A) Comparison of the reconstructed data (solid lines) with the predicted decay utilizing unidimensional exciton migration theory (points). (B) Comparison of the reconstructed data (solid lines) with the predicted decay utilizing confined domain theory.[36] Details of both theories are given in the text. The data correspond to intensities of 1.6×10^{10}, 5.7×10^{9}, 1.3×10^{9}, 3.6×10^{8}, and 1×10^{8} photons/cm^2 pulse (in descending order). All comparisons include convolution with a Gaussian instrument response (fwhm = 25 ps).

dynamics in colloidal chloroaluminum phthalocyanine.[40] This equation has also been applied to exciton annihilation in solid C_{60} where long-range, static Förster interactions occur in which case $h = {}^1/_2$.[37] The general solution to eq 3 is

$$[\mathrm{N}] = \frac{[\mathrm{N}]_0 \exp(-kt)}{1 + \left([\mathrm{N}]_0 \frac{\gamma}{2} k^{h-1} \Gamma(1-h,kt)\right)} \qquad (5)$$

where Γ is the incomplete gamma function ($h > 0$). Clearly, the above equation predicts non-Markovian exciton decay dynamics. Furthermore, this model is of interest since aggregate formation in PVS has been suggested to result in one-dimensional structures[10] and experiments on the temperature-dependent fluorescence quantum yield of BIC aggregates embedded in poly(vinyl alcohol) have suggested that the effective dimensionality of these aggregates is fractal with $d_f = 1.8$.[41]

To investigate the possibility of unidimensional or fractal exciton migration in PIC aggregates, the fluroescence decay data were modeled with eq 5 with the results for $h = {}^1/_2$ presented in Figure 3A. To compare eq 5 with the data, the data were reconstructed using the parameters from the biexponential fit (the "reconstructed data") with convolution to an instrument response modeled as a Gaussian with a fwhm of 25 ps. The integrated area of the fluorescence decay curves was also divided by the excited sample volume (1.25×10^{-6} cm^3) resulting in the absolute intensity scale depicted in Figure 3. Comparison was limited to intensities between 1×10^8 and 1.6×10^{10} photons/cm^2 pulse where the integrated fluorescence intensity was determined to be linear. Inspection of Figure 3A demonstrates that a one-dimensional model for the exciton migration is incapable of describing the observed excited-state decay. With a reduction in pulse energy, the theory predicts a turnover from biexponential to monoexponential decay at higher intensities than is observed. This result is consistent with recent NSOM experiments on PIC/PVS aggregates which demonstrate that the aggregates have a three-dimensional structure.[12] Further application of eq 5 for a range of dimensions was performed resulting in larger deviations from the experimental decays. Therefore, the exciton decay dynamics for PIC/PVS aggregates are not consistent with migration in fractal dimensions in contrast to BIC aggregates. This result is consistent with the structural differences between BIC and PIC aggregates as manifested in difference in absorption dichroism of these compounds.[15]

Exciton Migration in Restricted Domains. The theory for exciton decay when migration is limited to molecular domains of finite size was first presented by Paillotin et al. to describe the exciton dynamics in photosynthetic antenna pigments.[36] The assumptions inherent in this approach are that the exciton distribution is effectively randomized on a time scale shorter than the decay and that the excitons are confined to domains with no interaction between domains. This approach has been applied successfully to describe the power-dependent fluorescence quantum yield of PIC aggregates generated in aqueous solution.[30] The fluorescence decay is predicted to follow[36]

$$F(t) = \sum_{p=0}^{\infty} (-1)^p \exp(-(p+1)(p+r)\tau) A_p \qquad (6)$$

$$A_p = \sum_{m=p}^{\infty} \frac{(-1)^m m! Z^m (r+1+2p)}{p!\,(m-p)!(r+p+1)\ldots(r+p+1+m)} \qquad (7)$$

were $r = 2k/\gamma$, $\tau = \gamma t/2$, and Z is the number of excitons per domain. As has been noted, rigorous application of the above equations in modeling fluorescence decays is extremely difficult, although the limiting cases of $r = 0$ or $r =$ infinity are computationally facile to employ.[36] We can obtain an estimate of r to ascertain if a limiting form of the above equations can be employed by the following procedure. First, at the lowest powers the exciton decay dynamics follow single-exponential behavior providing a measure of the single exciton decay rate (0.00128 ps^{-1}). The exciton annihilation rate can be estimated by evaluating the slope of the fluorescence decay at early times, or by rearranging the binary collision equation into the form

$$\frac{1}{[\mathrm{N}]} \frac{\partial [\mathrm{N}]}{\partial t} = -k - \frac{\gamma}{2}[\mathrm{N}] \qquad (8)$$

demonstrating that a plot of $[\mathrm{N}]^{-1}\mathrm{d}[\mathrm{N}]/\mathrm{d}t$ versus $[N]$ should yield a line with a slope equal to $\gamma/2$ at early times. Application of this equation to our data results in an estimate for γ of 0.01 ± 0.05 ps^{-1} in agreement with previous estimates for PIC aggregates in water.[30,31] Therefore, $r \sim 0.2$ and a limiting form of eqs 6 and 7 is not applicable. Comparison of these equations to the reconstructed data (Figure 3B) was performed by expanding the summations and truncating the sum after the first two exponential terms (eq 6) and the first three prefactors for each exponential term (eq 7). In this treatment, only Z was adjusted and found to increase linearly up to 1×10^{10} photons/cm^2 pulse. Given the minimal expansion, the agreement between the predicted decay and the reconstructed data is remarkable. In contrast to reduced dimensionality theory, restricted domain theory predicts that annihilation should persist at much lower powers; however, single-exponential decays are recovered at lowest power.

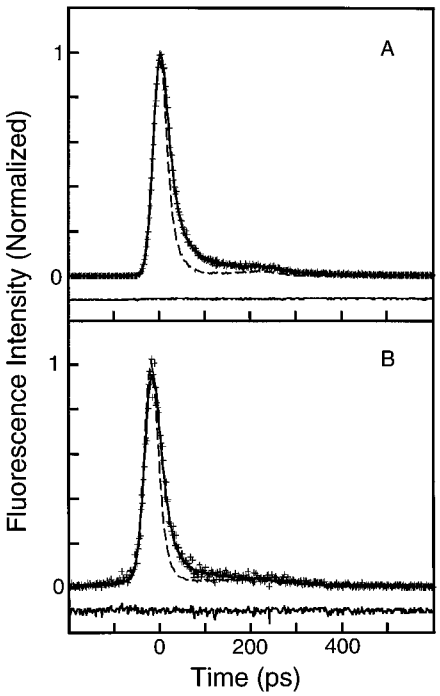

Figure 4. (A) Fluorescence decay observed for PIC/PVS aggregates deposited on a fused-quartz cover slip with TCSPC. The excitation intensity was 1.5×10^{12} photons/cm^2 pulse. Best fit to a convolution of the instrument response (dashed line) with a sum of two exponentials resulted in decay times of 8.5 ± 2.2 ps (0.95) and 70 ± 20 ps (0.05). Expansion of the residual difference between the data and the fit is given at the bottom of the figure. (B) Fluorescence decay of the same PIC/PVS samples as above obtained with the TCSPC-NSOM instrument. The excitation intensity was identical to that utilized above as measured in the far field. The decay time was identical to that measured above within the error of the measurement. Expansion of the residual difference between the data and the fit is given at the bottom of the figure.

Given the above comparisons, we conclude that the exciton decay kinetics for the PIC/PVS aggregates in solution are consistent with confinement to fixed domains. This result is in agreement with models in which exciton−phonon coupling limits the number of monomers that can support the exciton.[8,42,43] Furthermore, this conclusion is identical to previous conclusions derived from the power-dependent fluorescence quantum yield of PIC aggregates in aqueous solution.[30] However, the sensitivity of the fluorescence decay curves to exciton annihilation provides a more stringent test of annihilation theories. Finally, the failure of the unidimensional model in describing the power-dependent kinetics demonstrates that in the PIC/PVS system, exciton migration is not confined to a single dimension, suggesting that the aggregate structure in solution is more complicated that a single strand of chromophores attached to a linear, PVS backbone.

PIC Aggregates on Fused Quartz. In contrast to the excited-state decay kinetics observed for PIC/PVS aggregates in solution, deposition of the aggregates onto fused-quartz cover slips results in a dramatic increase in the excited-state decay rate. Figure 4A presents the fluorescence decay obtained for PIC/PVS aggregates spin-coated onto a fused-quartz coverslip (excitation intensity $= 1.6 \times 10^{12}$ photons/cm^2 pulse). The best fit to the data by a convolution of the instrument response with the sum of two exponentials results in decay time constants of 8.5 ± 2.5 ps (0.95) and 70 ± 20 ps (0.05) where the amplitudes of these time constants were insensitive to laser power. In contrast to the kinetics in solution, the decay is dominated by the short time constant. Furthermore, the power dependence of the aggregate/slide system is modest compared to the results in solution (Figure 2B). Power dependence of the short time constant was observed with this component decreasing from 17 ± 2 to 8.5 ± 2.5 ps between 3.6×10^8 and 1.6×10^{12} photons/cm^2 pulse, respectively. In agreement with previous studies of aggregates deposited onto silica surfaces, we assign the shorter time constant to the excited-state decay time.[44−47] Therefore, the modest power dependence observed for the PIC/PVS aggregates on quartz is due to the 80-fold increase in the single-exciton decay rate relative to the exciton−exciton annihilation rate.

The origin of the increased exciton decay rate for aggregates absorbed onto fused quartz is unclear. Previous studies of dye molecules and aggregates absorbed to metal, silver halide, and semiconductor surfaces have observed a similar reduction in the excited-state lifetime of the absorbed species and attributed this reduction to energy or electron transfer to the substrate.[7,48−50] However, the electronic transitions of silica are located in the ultraviolet, prohibiting efficient energy transfer for species which emit in the visible like the PIC/PVS aggregates studied here ($\lambda_{max} = 574$ nm[12]). Therefore, the increase in the excited-state decay rate cannot be ascribed to simple energy or electron transfer into the substrate.

An alternative explanation for the decrease in excited-state lifetime invokes excited-state "pseudodissociation" of the aggregate.[47] This mechanism was originally proposed to explain the excited-state decay kinetics of rhodamine B absorbed to fused quartz. In this mechanism, aggregation occurs on the surface of the quartz via molecule/substrate interactions with absorbed molecules forming aggregated structures. Photoexcitation of the aggregates leads to excited-state structural evolution, resulting in decomposition of the aggregate with the corresponding decay of the exciton. Since the molecules are "bound" to the silica surface, the aggregate is re-formed following internal conversion to the ground state. Although this mechanism may be operative in the PIC/PVS system, recent NSOM studies cast doubt on this hypothesis. NSOM measurements have revealed that the aggregate preparation utilized in these experiments results in ribbonlike aggregates with lengths >10 μm, widths of $\sim$200 nm, and thicknesses of $\sim$1−10 nm; different preparations result in dramatic differences in aggregate structure.[12,15,35] If aggregate formation were dominated by molecule/substrate interactions, one would expect to see a less dramatic preparation dependence of the aggregate structure, suggesting that the structure in solution is at least partially maintained during the spin-coating process. Therefore, we would expect to see exciton dynamics similar to those in solution. The large change in exciton decay kinetics between solution and quartz combined with the structural arguments presented above cast doubt on assigning the change in exciton dynamics to subsequent, substrate-induced aggregation following spin-coating.

Another possibility for enhanced exciton decay rate on fused quartz involves the presence of "sandwich dimer" sights created by the presence of the interface which act as energy sinks. The trapping of exciton energy by dimer structures embedded in the aggregate was originally proposed to explain the temperature and loading dependence of the exciton lifetime and fluorescence emission spectra for PIC aggregates attached to silver bromide crystals.[7] PIC dimers should have transitions located to the blue and red of the monomer absorption peak with the red shifted transition providing an energy trap.[7,51] If spin-coating results in perturbation of the aggregate structure such that dimers are formed at the quartz/aggregate interface, these dimers could act as energy sinks for the exciton providing a new, nonradiative decay mechanism. In previous investigations, the existence of

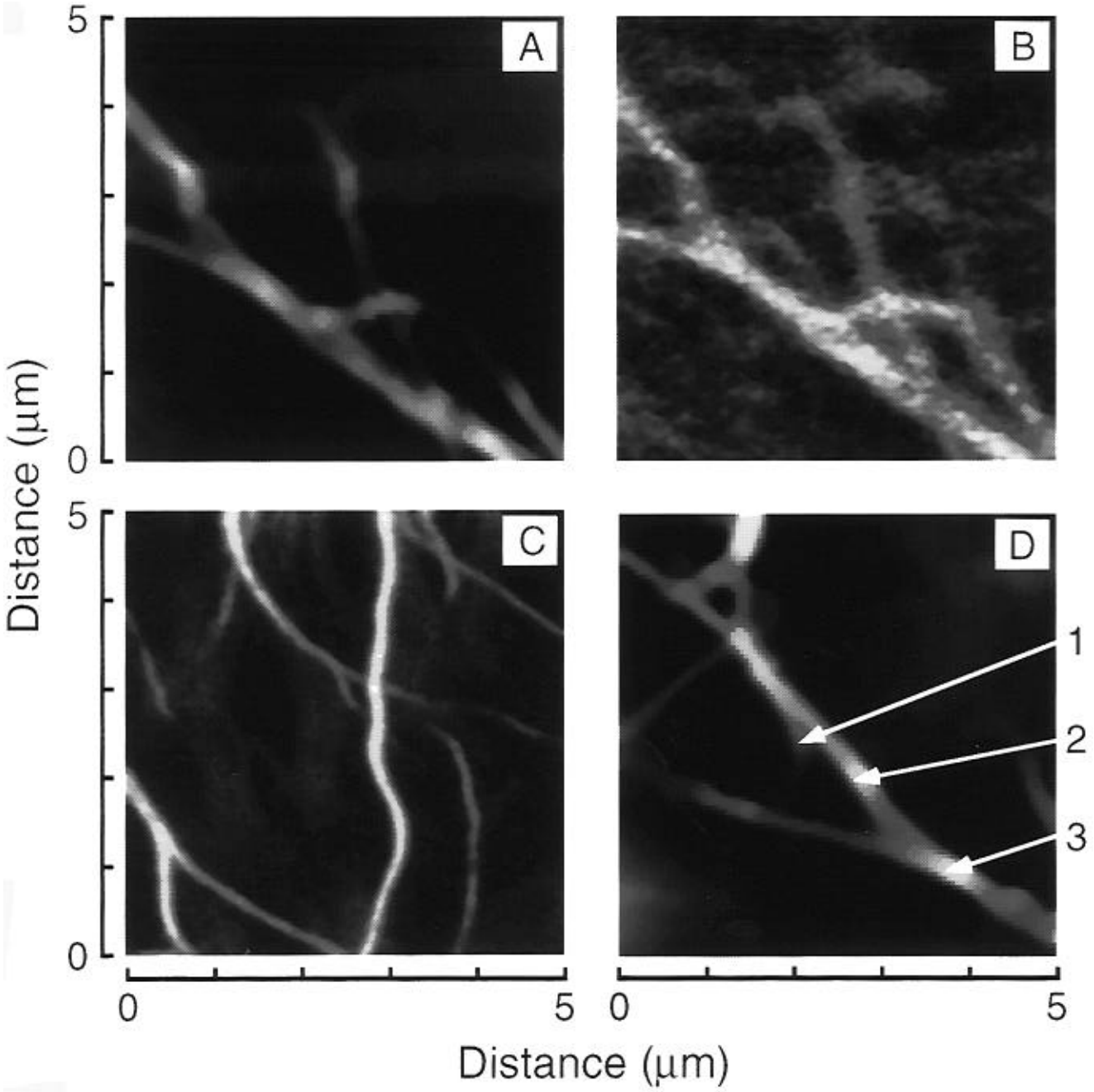

Figure 5. NSOM images of PIC/PVS aggregates. (A) Topographic image provided by the shear-force feedback of the NSOM tip. (B) Fluorescence NSOM image of the area identical to that depicted in A recorded with a multichannel plate detector. (C) Fluorescence NSOM image of a similar J-aggregate sample recorded with an avalanche photodiode detector. (D) Topographic image of the region where TCSPC-NSOM experiments were performed. The arrows on the figure indicate the different regions where the excited-state decay kinetics were investigated (see text).

dimers was manifested through the presence of a broad fluorescence peak red-shifted relative to emission from the J-band.[7] While the emission from J aggregates on fused quartz obtained with NSOM is consistent with emission from the J-band only,[12] the postulated sandwich dimer states may be present in small concentrations and may decay rapidly via nonradiative mechanisms. In summary, the exciton decay time for PIC/PVS aggregates on fused-quartz substrates decreases by ~80 times relative to solution; however, the mechanism responsible for this rate enhancement remains unclear.

NSOM of PIC Aggregates on Fused Quartz. In designing the TCSPC-NSOM instrument, a few technical concerns arise, the most important being the requirement to resolve the ~10 ps exciton decay dynamics for the aggregates on fused quartz. Previous TCSPC-NSOM designs utilized a low-bias avalanche photodiode (AP) configured for fast response resulting in an IRF of 120 ps fwhm.[24] However, this instrument would not have sufficient temporal resolution to resolve the kinetics of interest here. Therefore, we replaced the AP with a multichannel plate (MCP) and the corresponding electronics utilized in the far-field TCSPC experiments. Figure 5 presents images of the aggregates obtained with the NSOM instrument. Figure 5A depicts a topographic image of the sample obtained via the shear-force mechanism.[52] Figure 5B presents the simultaneously-recorded fluorescence NSOM images of the same area excited at 570 nm. The fluorescence was detected with the MCP and was recorded by monitoring the "true-start" output of the TAC which provides a convenient TTL source of the detector output (the discriminated output of the MCP serves as the start-pulse in reverse-timing mode). The resolution and S/N of the images displayed here compare favorably with our previous results.[12,15] An image of a different sample of the PIC/PVS aggregates

recorded with an AP detector is shown in Figure 5C for comparison. A reduction in the S/N of the NSOM images is observed with this instrument due to the reduction in photocathode quantum efficiency between the AP ($\phi \approx 0.4$) and the MCP ($\phi \approx 0.08$) at this wavelength.

With the characterization of the exciton dynamics of the PIC/PVS aggregates provided by far-field TCSPC, we applied TCSPC-NSOM to investigate the dependence of the exciton decay dynamics on the nanometric structural features of the aggregates. The fluorescence decay from a PIC/PVS aggregate obtained with the TCSPC-NSOM instrument is presented in Figure 4B (intensity = 1.6×10^{12} photons/cm^2 pulse). *This represents the first measurement of the exciton decay dynamics for an individual aggregate*. The figure also presents the 30 ps fwhm IRF of the instrument. The intensity dependence of the exciton decay as determined by TCSPC-NSOM is presented in Figure 2B (squares). To compare the near-field and far-field TCSPC results, the excitation intensities employed in the NSOM experiments (and used to plot the NSOM data in Figure 2B) were measured in the far field. However, field-enhancement effects in NSOM have been proposed; therefore, this comparison should be viewed as tentative.[24,29] Given this caveat, the excited-state lifetimes measured by TCSPC-NSOM are in remarkably good agreement with conventional TCSPC, suggesting that tip enhancement/fluorescence quenching effects are of minimal importance in these particular experiments.

The dependence of the exciton decay on the structure of the aggregate was determined by measurement of the fluorescence decay at various locations. Figure 5D depicts the three aggregate structures that were investigated: single aggregates (1), aggregate bundles (2), and aggregate intersections (3). At the intensity employed in this study (1.6×10^{12} photons/cm^2 pulse), dependence of the decay kinetics on aggregate structure was not observed with all locations resulting in a decay time of ~8.5 ps. This result suggests that the exciton decay kinetics are homogeneous, similar to the fluorescence spectra.[12] We can use this information to construct a picture of exciton migration in the PIC/PVS aggregates. Length scales for migration can be estimated by a Förster type energy-transfer calculation in the limit of incoherent, percolative motion. First, since the exciton migration occurs from one set of coupled monomers to a neighboring group, we can envision our system as a set of chromophores at high concentration. In this limit, the exciton migration in three dimensions can be described as diffusive with the average displacement related to the diffusion constant by

$$\langle X^2 \rangle_t = 6Dt \tag{9}$$

where X is the displacement and D is the diffusion constant.[53,54] The diffusion constant is related to the Förster characteristic transition distance (R_0, assuming simple cubic packing of the excitonic sites) by

$$D = 0.409C^{4/3}R_0{}^2\tau^{-1} \tag{10}$$

where C is the reduced concentration equal to $4\pi R_0{}^3\rho/3$ (ρ is the exciton density), and τ is the exciton lifetime. With substitution, the mean-square displacement in one lifetime becomes

$$\langle X^2 \rangle = 2.45[4\pi\rho/3]^{4/3}R_0{}^6 \tag{11}$$

Estimates for the number of monomers which are coupled in formation of an exciton vary from 4 to 20; therefore, we assume an average value of 10 in evaluating the above equations.[8] If one molecule takes up ~250 Å^3 (10 Å × 5 Å × 5 Å) then the exciton density is $(10 \times 250$ Å$^3)^{-1}$ or 4×10^{-4} Å^{-3}. All that remains in evaluation of eq 11 is a value for R_0 which can be determined with the following equation:[55]

$$R_0{}^6 = \frac{162K^2\Phi_f}{\pi^5 n^4 N_A}\int_0^\infty \frac{f(\nu)\,\epsilon(\nu)}{\nu^4}\,\partial\nu \text{ (cm}^6\text{)} \tag{12}$$

where K is the dipole orientation factor (4 for aligned donor−acceptor systems), Φ_f is the fluorescence quantum yield of an isolated exciton, n is the refractive index, N_A is Avagadro's number, and the integration is of the product of the normalized fluorescence spectrum and the extinction coefficient weighted by the fourth power of frequency. An estimate for the fluorescence quantum yield for the aggregates on fused quartz can be obtained by assuming that the quantum yield in solution is 0.5 and that the 80 fold reduction in exciton lifetime when the aggregates are deposited onto fused quartz is due to nonradiative processes yielding $\Phi_f = 0.006$. This estimate is reasonable in light of the 0.02 emission quantum yield obtained for a different preparation of PIC/PVS aggregates in solution.[10] An estimate for ϵ was obtained by assuming that the concentration of aggregates giving rise to a maximum absorbance of 0.1 in a 100 μm cell is a factor of 10 less that the monomer concentration, consistent with the above exciton density calculation. This results in $\epsilon = 160\,000$ M^{-1} cm^{-1} consistent with previous measurements of ϵ for PIC aggregate films on glass.[56] Using this value, the integration produces a value of 1×10^{-13} cm^6/M. Finally, estimating $n = 1.5$, the evaluation of eq 13 results in $R_0 = \sim$40 Å. Typical values for donor−acceptor systems demonstrating efficient energy transfer range between 5 and 50 Å;[57] therefore, this estimate is not unreasonable given the minimal Stokes shift of the emission in PIC aggregates.

Utilizing the estimate for R_0 and ρ, evaluation of eq 11 results in a diffusion length of 140 nm in one exciton lifetime in agreement with previous estimates.[1] This represents an upper limit to the diffusion length since trapping sites, exciton annihilation, and disorder between coupled molecules supporting the exciton have not been included in this analysis. The ~100 nm estimate for the diffusion length is consistent with our previous NSOM studies of photochemical hole-burning and emission dichroism in PIC/PVS aggregates.[12,15] In both of these studies, an upper limit of 50 nm was suggested for the exciton migration length. The TCSPC-NSOM results add to these studies by identifying the origin of the limited exciton diffusion length, namely, the short exciton lifetime.

A final conclusion can be drawn from comparison of the previous and current NSOM results. The spectrally and temporally resolved fluorescence data demonstrate that the aggregate photophysical properties are consistent with a homogeneous aggregate structure. Previous rational for the homogeneity of aggregate emission was based on efficient migration of the exciton which would average site inhomogeneities. However, the TCSPC-NSOM results presented here demonstrate that the excitons migrate over very short distances; therefore, the homogeneous nature of the J-aggregate emission is not due to efficient migration but is instead due to the homogeneity of the aggregate structure on the length scales investigated here. This is the identical conclusion reached from analysis of the linear dichroism of the PIC/PVS aggregates obtained with NSOM.[15] However, inhomogeneity in the aggregate structure must exist on length scales smaller than those investigated here since the J-band is inhomogeneously broadened as demonstrated by low-temperature spectral hole-burning.[34,58]

Conclusions

In this paper, we have performed time-resolved fluorescence spectroscopy on PIC aggregates embedded in PVS in various environments utilizing conventional TCSPC as well as TCSPC-NSOM. The single exciton lifetime in solution was observed to be ~800 ps, consistent with previous studies on PIC aggregates in aqueous solution. Similarly, exciton annihilation was observed at elevated excitation intensities, as in the previous studies. The power-dependent decay kinetics were modeled with conventional exciton decay theories and found to be consistent with exciton migration constrained to finite domains. Deposition of the PIC/PVS aggregates onto fused-quartz results in a dramatic reduction in the exciton lifetime to ~10 ps. TCSPC-NSOM was performed to determine the dependence of exciton lifetime on the structural details of the aggregate with no dependence observed. Finally, the photophysical properties of PIC/PVS aggregates were analyzed and demonstrate that due to the limited exciton diffusion length, the homogeneity of the spectral and temporal properties of the PIC/PVS fluorescence must arise from a homogeneous aggregate structure on length scales of 100 nm and larger.

Acknowledgment. The authors would like to thank the Office of Naval Research, the National Science Foundation (CHE-9304373), and the University of Minnesota for financial support. D.A.H. was supported by a postdoctoral fellowship from the National Science Foundation. Finally we would like to thank Susan Dexheimer, currently at Los Alamos National Labs, for helpful discussions and assistance in the derivation of eq 5.

References and Notes

(1) Möbius, D. *Adv .Mater*. **1995**, *7*, 437.
(2) Bohn, P. W. *Annu. Rev. Phys. Chem*. **1993**, *44*, 37.
(3) Herz, A. H. *Adv. Colloid Interface Sci*. **1977**, *8*, 237.
(4) Scheibe, G. *Angew. Chem*. **1936**, *49*, 563.
(5) Jelley, E. E. *Nature* **1936**, *138*, 1009.
(6) James, T. H. *The Theory of the Photographic Process*, 4th ed.; Macmillan Publishing Co.: New York, 1966.
(7) Muenter, A. A.; Brumbaugh, D. V.; Apolito, J.; Horn, L. A.; Spano, F. C.; Mukamel, S. *J. Phys. Chem*. **1992**, *96*, 2783.
(8) Spano, F. C.; Kuklinski, J. R.; Mukamel, S. *J. Chem. Phys*. **1991**, *94*, 7534.
(9) Minoshima, K.; Taiji, M.; Misawa, K.; Kobayashi, T. *Chem. Phys. Lett*. **1994**, *218*, 67.
(10) Horng, M.-L.; Quitevis, E. L. *J. Phys. Chem*. **1993**, *97*, 12408.
(11) Knapp, E. W. *Chem. Phys*. **1984**, *85*, 73.
(12) Higgins, D. A.; Barbara, P. F. *J. Phys. Chem*. **1995**, *99*, 3.
(13) Emerson, E. S.; Conlin, M. A.; Rosenoff, A. E.; Norland, K. S.; Rodriguez, H.; Chin, D.; Bird, G. R. *J. Phys. Chem*. **1967**, *71*, 2396.
(14) Wolthaus, L.; Schaper, A.; Mobius, D. *Chem. Phys. Lett*. **1994**, *225*, 322.
(15) Higgins, D. A.; Reid, P. J.; Barbara, P. F. *J. Phys. Chem*. **1996**, *100*, 1175.
(16) Betzig, E.; Trautman, J. K.; Harris, T. D.; Weiner, J. S.; Kostelak, R. L. *Science* **1991**, *251*, 1468.
(17) Betzig, E.; Trautman, J. K. *Science* **1992**, *257*, 189.
(18) Betzig, E.; Chichester, R. J. *Science* **1993**, *262*, 1422.
(19) Harris, T. D.; Grober, R. D.; Trautman, J. K.; Betzig, E. *Appl. Spectrosc*. **1994**, *48*, 14A.
(20) Trautman, J. K.; Macklin, J. J.; Brus, L. E.; Betzig, E. *Nature* **1994**, *369*, 40.
(21) Grober, R. D.; Harris, T. D.; Trautman, J. K.; Betzig, E.; Wegscheider, W.; Pfeiffer, L.; West, K. *Appl. Phys. Lett*. **1994**, *64*, 1421.
(22) Ambrose, W. P.; Goodwin, P. M.; Martin, J. C.; Keller, R. A. *Science* **1994**, *265*, 364.
(23) Dunn, R. C.; Holtom, G. R.; Mets, L.; Xie, X. S. *J. Phys. Chem*. **1994**, *98*, 3094.
(24) Xie, X. S.; Dunn, R. C. *Science* **1994**, *265*, 361.
(25) Lieberman, K.; Harush, S.; Lewis, A.; Kopelman, R. *Science* **1990**, *247*, 59.
(26) Birnbaum, D.; Kook, S.-K.; Kopelman, R. J. *J. Phys. Chem*. **1993**, *97*, 3091.
(27) Vaez-Iravani, M.; Toledo-Crow, R. *Appl. Phys. Lett*. **1993**, *62*, 1044.
(28) Vigoureux, J. M.; Depasse, F.; Girard, C. *Appl. Opt*. **1992**, *31*, 3036.
(29) Dürig, U.; Pohl, D. W.; Rohner, F. *J. Appl. Phys*. **1986**, *59*, 3318.
(30) Sundstrom, V.; Gillbro, T.; Gadonas, R. A.; Piskarskas, A. *J. Chem. Phys*. **1988**, *89*, 2754.
(31) Brumbaugh, D. V.; Muenter, A. A.; Knox, W.; Mourou, G.; Wittmershaus, B. *J. Lumin*. **1984**, *31* and *32*, 783.
(32) Dorn, H.-P.; Mueller, A. *Appl. Phys. B* **1987**, *43*, 167.
(33) Bevington, P. R. *Data Reduction and Error Analysis for the Physical Sciences*; McGraw-Hill: New York, 1976.
(34) Misawa, K.; Machida, S.; Horie, K.; Kobayashi, T. *Chem. Phys. Lett*. **1995**, *240*, 210.
(35) Higgins, D. A.; Kerimo, J. K.; Vanden Bout, D. A.; Barbara, P. F. *J. Am. Chem. Soc*., submitted.
(36) Paillotin, G.; Swengerg, C. E.; Breton, G.; Gencintov, N. E. *Biophys. J*. **1979**, *25*, 513.
(37) Dexheimer, S. L.; Vareka, W. A.; Mittleman, D.; Zettl, A.; Shank, C. V. *Chem. Phys. Lett*. **1995**, *235*, 552.
(38) Kopelman, R.; Parus, S.; Prasad, J. *Phys. Rev. Lett*. **1986**, *56*, 1742.
(39) Klymko, P. W.; Kopelman, R. *J. Phys. Chem*. **1983**, *87*, 4565.
(40) Gubinas, V.; Chachisvilis, M.; Persson, A.; Svanberg, S.; Sundstrom, V. *J. Phys. Chem*. **1994**, *98*, 8118.
(41) Kamalov, V.; Yoshihira, K. Self-trapping of Low-dimensional Aggregates of Carbocyanine Dyes; Time-Resolved Vibrational Spectroscopy-7, 1995, Santa Fe, NM.
(42) Boer, S. D.; Wiersma, D. A. *Chem. Phys. Lett*. **1990**, *165*, 45.
(43) Fidder, H.; Knoester, J.; Wiersma, D. A. *Chem. Phys. Lett*. **1990**, *171*, 529.
(44) Quitevis, E. L.; Horng, M.-L.; Chen, S.-Y. *J. Phys. Chem*. **1988**, *92*, 256.
(45) Horng, M.-L.; Quitevis, E. L. *J. Phys. Chem*. **1989**, *93*, 6198.
(46) Chen, S.-Y.; Horng, M.-L.; Quitevis, E. L. *J. Phys. Chem*. **1989**, *93*, 3683.
(47) Kemnitz, K.; Yoshihara, K.; Tani, T. *J. Phys. Chem*. **1990**, *94*, 3099.
(48) Anfinrud, P. A.; Causgrove, T. P.; Struve, W. S. *J. Phys. Chem*. **1986**, *90*, 5887.
(49) Crackel, R. L.; Struve, W. S. *Chem. Phys. Lett*. **1985**, *102*, 473.
(50) Tani, T.; Suzumoto, T.; Kemnitz, K.; Yoshihara, K. *J. Phys. Chem*. **1992**, *96*, 2778.
(51) McRae, E. G.; Kasha, M. *J. Chem. Phys*. **1958**, *28*, 721.
(52) Betzig, E.; Finn, P. L.; Weiner, J. S. *Appl. Phys. Lett*. **1992**, *60*, 2484.
(53) Gochanour, C. R.; Andersen, H. C.; Fayer, M. D. *J. Chem. Phys*. **1979**, *70*, 4254.
(54) Haan, S. W.; Zwanzig, R. *J. Chem. Phys*. **1978**, *68*, 1879.
(55) Cantor, C. R.; Schimmel, P. R. *Biophysical Chemistry*; W. H. Freemen and Co.: San Francisco, 1980; Vol. II.
(56) Scherer, P.; Kopainsky, B.; Kaiser, W. *Opt. Commun*. **1981**, *39*, 375.
(57) Berlman, I. B. *Energy Transfer Parameters of Aromatic Compounds*; Academic Press: New York, 1973.
(58) Boer, S. D.; Vink, K. J.; Wiersma, D. A. *Chem. Phys. Lett*. **1987**, *137*, 99.

JP953033N